

IJPGC2003-401152**DEVELOPMENT OF A THERMAL APPROACH TO OPTIMIZE THE WASTE
HEAT UTILIZATION FROM AN EXISTING GAS TURBINE STATION
WITHOUT HEAT RECOVERY SYSTEM****Guyh Dituba Ngoma****University of Quebec in Abitibi-Temiscamingue
Department of Applied Sciences
445, Boulevard de l'Université
Rouyn-Noranda, Quebec, J9X 5E4, Canada
guyh.dituba-ngoma@uqat.ca****Amsini Sadiki****Darmstadt University of Technology
Department of Energy and Power Plant Technology
Petersenstrasse 30
64287 Darmstadt, Germany****ABSTRACT**

The present work deals with a numerical simulation of a flow in finned tube banks arranged behind a gas turbine. Three models of dual-pressure tube systems are developed and analyzed in order to predict the static system performances by optimizing the utilization of the exhaust gas from an existing gas turbine without heat recovery system. For more precise modeling, the theoretical analysis of finned tube banks systems is based on the non-linear conservation equations of mass, momentum and energy. Simulations are accomplished to prove the effectiveness of the present work in performance prediction of the dual-pressure tube systems. The obtained results clearly show the necessity to take into account all relevant physical phenomena in the simulation of flows in and across finned tube banks installed behind a gas turbine. The results also reveal the different operating behavior of the developed models considering combined effects of the exhaust gas parameters and the tube geometries.

KEY WORDS

Power system, Combined Cycle, Steam generators, Gas Turbines, Steam Turbines, Modeling and Simulation

INTRODUCTION

In the concept of the global trend to deregulate the energy market and to reduce the environmental pollution problems, nowadays, flow heat exchangers are extensively installed behind an existing gas turbine station, e.g. gas turbine for compressor station [1-3]. This allows to recovery the waste heat contained in the exhaust hot gas from gas turbines. In the practise, especially for existing gas turbines without heat recovery system, many flow arrangements can be used for the heat transfer between working fluid and exhaust gas. Here, the working fluid flows in finned tube banks and the exhaust gas

pass across them. The produced steam is needed for the steam turbine in order to drive a electrical generator. This contributes to enhance the system overall efficiency [4-5]. The tube banks arrangements strongly depend on the space available behind the gas turbine. For dual-pressure systems, there are the parallel and serial configurations of tube banks. In the parallel flow tube banks, the exhaust gas gives heat to two water flows at the same time. In the serial configuration, the exhaust gas sequentially gives heat to the first and second tube banks [6]. These tube banks have a compact construction and its configuration plays an important role for the system performances including the optimal utilization of the exhaust gas, the reliability and the safety of power plant operations. The investigation of this system behavior is also considered in the planning and design steps of power plants in order to improve system static and dynamic performances in the operating phase. The purpose of this work is to develop an approach, which allows to optimise the utilization of the exhaust gas from an existing gas turbine without any heat recovery system. Here, the concept of the dual-pressure levels on the work fluid side is considered [4,7]. Three configurations of tube banks systems are analysed and compared. Since the heat transfer in heat recovery processes is mainly convective, the present study takes into consideration the variation of the heat surface load along the once-through tubes. For more precise analysis, non-linear mathematical system of equations are established in modeling process. There, the two-phase steam/water flow is simulated with the drift flux model according to the Rouhani correlation. This allows to take into account the velocities of water and steam phases [8-9]. The influence of the tube geometries and the tube walls on the system thermal performances are examined. Also, the effects of the exhaust gas parameters on the flow-fields of the working fluid are analysed.

NOMENCLATURE

• Symbols

A	tube cross sectional area
c	specific heat
d	diameter
g	acceleration due to gravity
h	enthalpy
\dot{m}	mass flow rate
p	pressure
r	vaporization heat
t	time
U	tube circumference
u	internal energy
w	flow velocity
\dot{x}	steam quality
z	distance
α	convection heat transfer coefficient
β	tube orientation angle from the horizontal
ε	void fraction
ϑ	temperature
ρ	density

• Subscripts

G	steam phase
L	water phase
R	friction pressure drop
w	tube wall
wf	working fluid
hg	hot gas

2. SYSTEM DESCRIPTION

Fig. 1 shows the first and second considered models of once-through heat recovery steam generator (HRSG) with two pressure levels. The third investigated models are represented in Fig. 2. The models 1 and 2 are characterized by

$$\dot{m}_{hg1} = \dot{m}_{hg2} = \frac{\dot{m}_{hg}}{2} \quad \text{and} \quad \dot{m}_{hg1} \neq \dot{m}_{hg2} \quad \text{respectively.}$$

The three models mainly consist of two once-through systems in counter current flow and a gas turbine with a vertical path for the exhaust gas. The finned tube banks are used in order to improve the heat transfer efficiencies. Preheating, evaporation and superheating consecutively take place in finned tube banks. Therefore, the position of the water-to-steam interface is free to move through the tube banks, depending on the heat input from the exhaust gas, the mass flow rate and pressure of the feedwater.

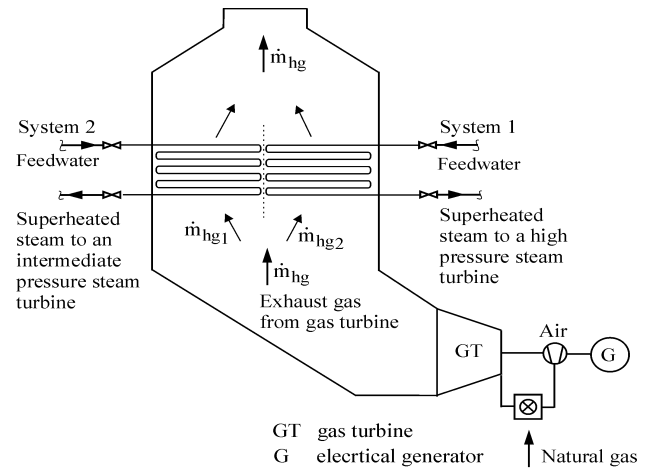


Figure 1: Dual pressure once-through HRSG systems in parallel configuration

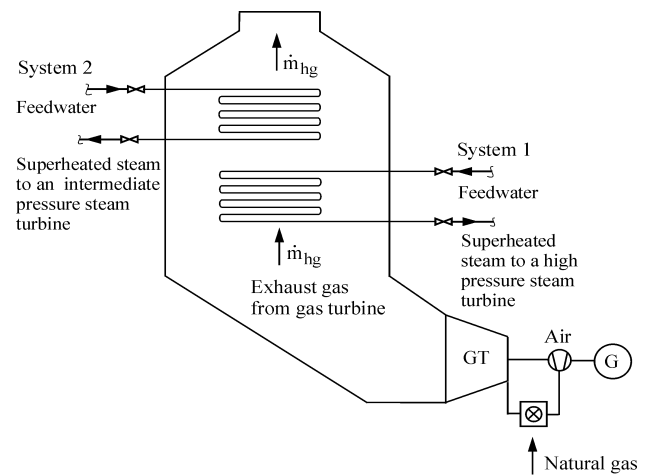


Figure 2: Dual pressure once-through HRSG systems in serial configuration

3. SYSTEM MODELING

The theoretical analysis of the once-through HRSG systems given in Figs. 1-2 is based on the conservation equations of mass (1-2), momentum (3-4), energy (5-7) for exhaust gas (only single-phase flow), working fluid (single- and two-phase flow) and tube wall [10-11]. For the single-phase flow, the mass conservation is given by:

$$\frac{\partial \rho}{\partial t} + \frac{\partial (\rho w)}{\partial z} = 0 \quad (1)$$

and for the two-phase flow, it can be written as follows:

$$\begin{aligned} & \frac{\partial}{\partial t} (\rho_L (1 - \varepsilon) + \rho_G \varepsilon) \\ & + \frac{\partial}{\partial z} (\rho_L (1 - \varepsilon) w_L + \rho_G \varepsilon w_G) = 0 \end{aligned} \quad (2)$$

where symbols and subscripts are defined in the nomenclature. The momentum conservation for the single-phase flow is defined by:

$$\frac{\partial(\rho w)}{\partial t} = -\frac{\partial(\rho w^2)}{\partial z} - \rho g \sin \beta - \frac{\partial p}{\partial z} - \left. \frac{\partial p}{\partial z} \right|_R \quad (3)$$

and for the two-phase flow, it can be given by:

$$\begin{aligned} & \frac{\partial}{\partial t} (\rho_L (1-\varepsilon) w_L + \rho_G \varepsilon w_G) \\ & + \frac{\partial}{\partial z} (\rho_L (1-\varepsilon) w_L^2 + \rho_G \varepsilon w_G^2 + p) \\ & + (\rho_L (1-\varepsilon) + \rho_G \varepsilon) g \sin \beta + \left. \frac{\partial p}{\partial z} \right|_R = 0 \end{aligned} \quad (4)$$

The energy conservation for the single-phase flow is described by:

$$q \frac{U}{A} + \frac{\partial}{\partial t} p = \frac{\partial}{\partial t} (\rho h) + \frac{\partial}{\partial z} (\rho w h) \quad (5)$$

and for the two-phase flow, it is given by:

$$\begin{aligned} q \frac{U}{A} + \frac{\partial p}{\partial t} &= \frac{\partial}{\partial t} (\rho_L (1-\varepsilon) E_L + \rho_G \varepsilon E_G) \\ &+ \frac{\partial}{\partial z} (\rho_L (1-\varepsilon) E_L w_L + \rho_G \varepsilon E_G w_G) \end{aligned} \quad (6)$$

where $E_k = h_k + \frac{w_k^2}{2} + gz \sin \beta$; $k = L, G$ and $q = \alpha(\vartheta_w - \vartheta)$

The tube wall energy conservation can be written as follows:

$$\begin{aligned} c_w \rho_w \frac{\partial \vartheta_w}{\partial t} &= \alpha_{hg} U_{hg} (\vartheta_{hg} - \vartheta_w) \\ &+ \alpha_{wf} U_{wf} (\vartheta_{wf} - \vartheta_w) \end{aligned} \quad (7)$$

The previous system of partial differential equations has been numerically solved. Therefore, the difference finite scheme (spatial and temporal discretization) is used to obtain the mass flow rate, the pressure and the temperature for the single-phase or the steam quality for the two-phase flow. The recuperator model has been used to take into consideration the coupling of the exhaust gas and the working fluid sides with the tube wall [12]. For numerical solutions, the dual-pressure once-through HRSG model is based on equidistant increments (space and time). The numerical calculations of the state and the thermodynamic values are performed on a sequential base. Additionally, the constitutive equations are considered in the calculations [11,13-15].

4. SIMULATION RESULTS AND DISCUSSIONS

As boundary conditions for the system behavior investigations, the mass flow rate and the temperature on the working fluid side are considered as constant at the inlet of both systems. The gas turbine components are not simulated. The consideration of the exhaust gas parameters in the calculations is accomplished from the outlet of the gas turbine. This outlet is characterized by the exhaust gas state, i.e., the mass flow rate, the temperature, the pressure, the concentration of CO₂ and the humidity of the exhaust gas. To calculate the thermodynamic state of the exhaust gas, a program in FORTRAN 90 is developed using the polynomial functions in [16] which depend on the temperature. This program allows to determinate, for the exhaust gas, the enthalpy, the specific heat, the thermal conductivity, the dynamic viscosity, the Prandtl number for dry air by 1 bar. The specific volume is calculated using the ideal gas perfect relation. The properties of water and steam are calculated by means of a written program in FORTRAN 90 using the water and steam relations in [17]. For the main model calculations, a high and intermediate pressure levels of 105 bar and 25 bar are chosen for the systems 1 and 2 respectively for the three examined models. The mass flow rates on the exhaust gas side are 200 kg/s for the models 1 and 2 as well as 220 kg/s for the model 3. The temperature of the exhaust gas is 560°C. Furthermore, in order to validate the developed model, the available experimental data from a single pressure once-through HRSG test facility are compared with the achieved simulation results corresponding in the single pressure case. Fig. 3 clearly shows a good agreement between the numerical results and experimental data for the temperature distribution along the considered single pressure once-through tube.

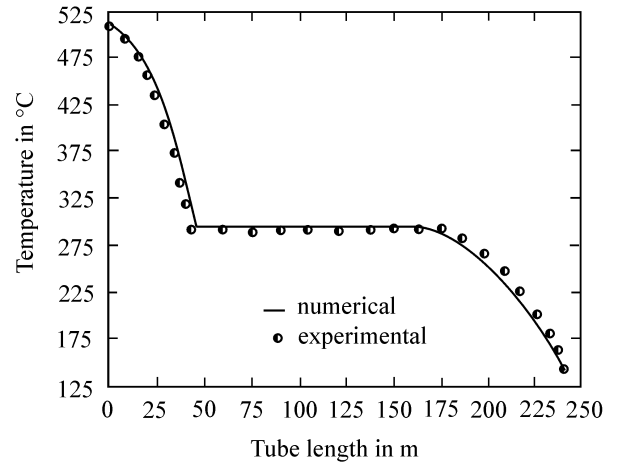


Figure 3: Temperature versus tube length

4.1 Effect of the tube length

In order to investigate the effect of the tube length on the outlet exhaust gas and working fluid parameters, the tube diameter is kept constant with the values of 0.038 mm and 0.0316 mm for the inner and outer diameters respectively. In the model 1, Fig. 4 shows the decreasing outlet exhaust gas temperature with increasing tube length. In this analyzed case, an augmentation of the tube length of 54.55% from 100 m leads to a reducing of the average outlet exhaust gas temperature of 13.8%. The exhaust gas temperature decreasing

is greater for the system 2 than that for the system 1. The corresponding curves of the density and steam quality as function of the tube length are represented in Figs. 5-6. There, its variations are shown within the tube inlet and outlet for both systems.

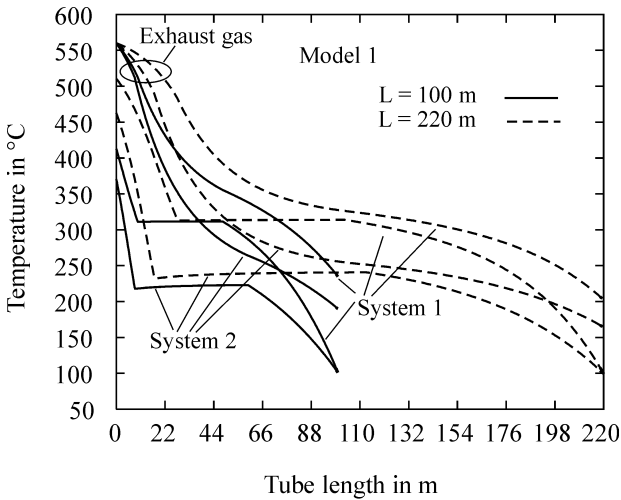


Figure 4: Temperature versus tube length

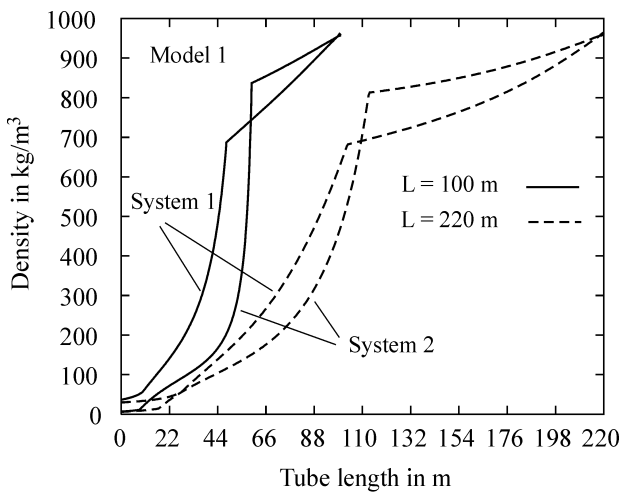


Figure 5: Density versus tube length

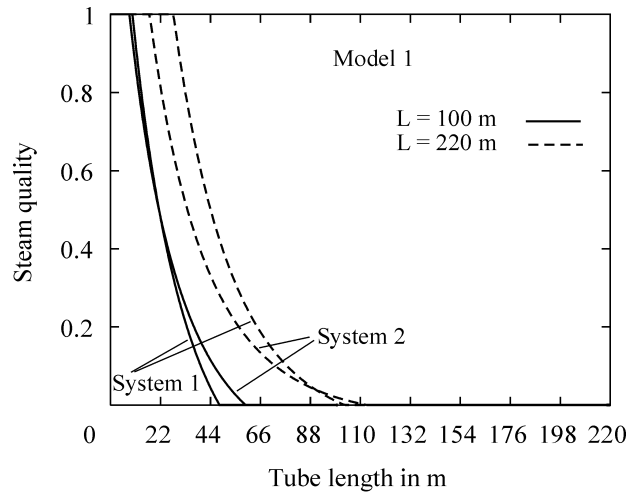


Figure 6: Steam quality versus tube length

Concerning the model 2 with a distribution of the exhaust gas mass flow rate of 45% for the system 1 and 55% for the system 2, Fig. 7 presents the variation of the temperatures on the exhaust gas and working fluid sides as function of the tube length. It can be observed that 54.55% increasing tube length of leads to a decreasing average outlet exhaust gas temperature of 14.8%. Moreover, the systems 1 and 2 have almost the same exhaust gas temperature at the outlet.

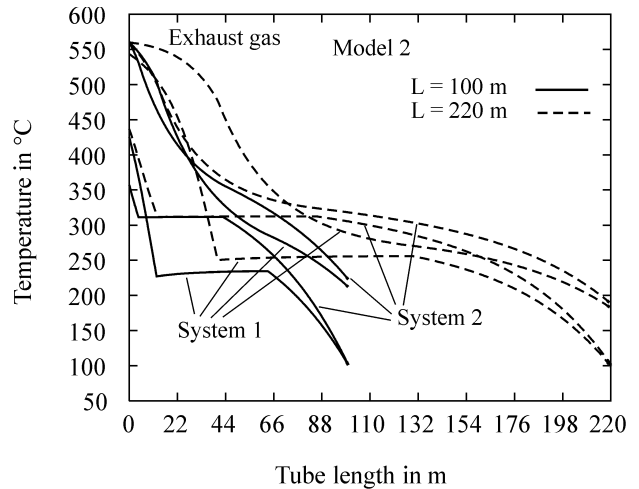


Figure 7: Temperature versus tube length

Regarding the model 3, Figs. 8-9 present the temperature and the density as function of the tube length. From Fig. 8, it is clearly shown that the tube length strongly plays an important role in the reducing of the outlet exhaust gas temperature which corresponds of a decrease of 17.8% from 265.2°C. Also, the working flow parameters depend of the tube length as shown in Figs. 8-9.

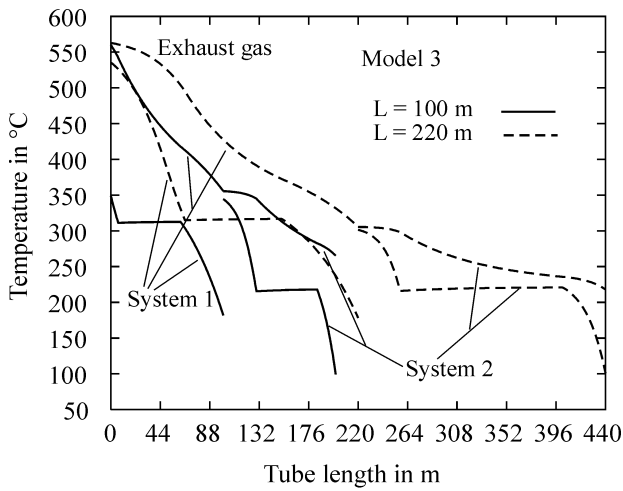


Figure 8: Temperature versus tube length

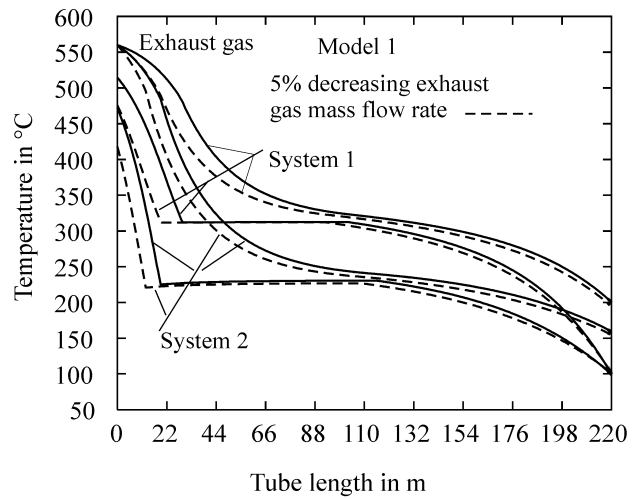


Figure 10: Temperature versus tube length

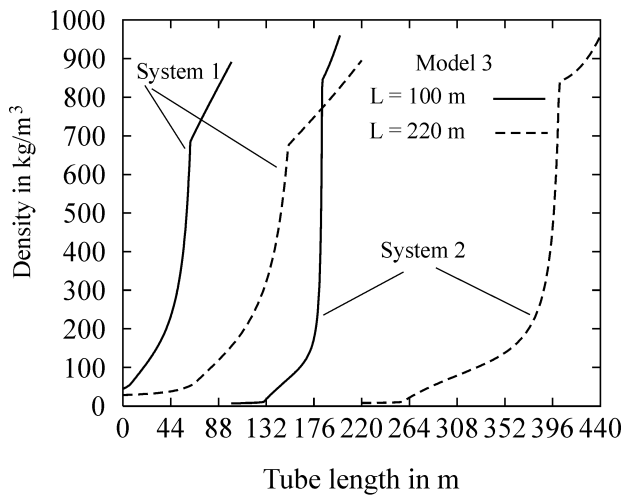


Figure 9: Density versus tube length

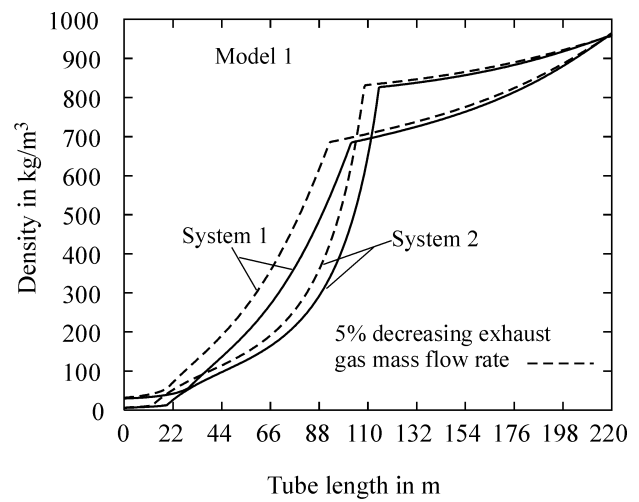


Figure 11: Density versus tube length

4.2 Effect of decreasing exhaust gas mass flow rate

In order to analyze the effect of a reducing of the exhaust gas mass flow rate on the working fluid parameters, the exhaust gas temperature is kept constant and the mass flow rate is reduced of 5% from 200 kg/s for the model 1 and 3.2% from 220 kg/s for the model 3. The reducing exhaust gas mass flow rate in the model 1 leads to a decreasing outlet working fluid temperature of 7.5% from 514.5°C and 11.4% from 471.8°C for the systems 1 and 2 respectively. Also, the average outlet exhaust gas temperature decreases of 2.9% from 179.7°C as shown in Fig. 10. In addition, from this figure, it can be observed the displacement of the boiling end point to the tube outlet for both systems. In this considered case, the outlet density on the working fluid side is almost constant for both systems, while the variation of the density between the tube inlet and outlet is observed as represented in Fig. 11. The corresponding steam quality curve is shown in Fig. 12 for both systems.

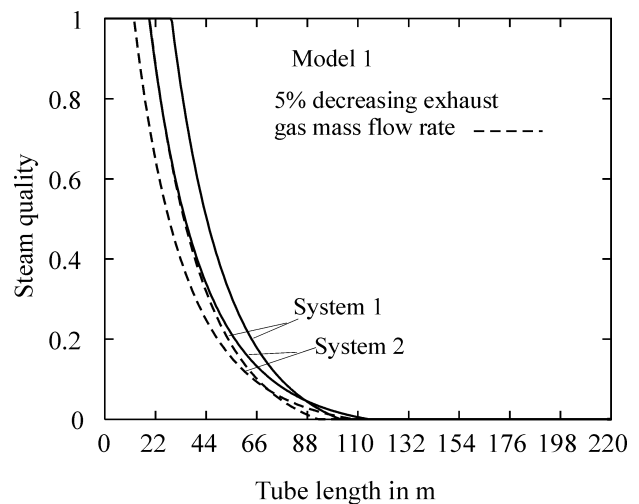


Figure 12: Steam quality versus tube length

In the model 2, the previous observed tendencies in the model 1 are similar as represented in Fig. 13 for the case of the

temperature variation as function of the tube length. There, it is clearly to remark the effect of an unequal distribution of the exhaust gas mass flow rate on the working fluid temperatures which decrease of 7.7% from 440°C and 7.1% from 550.8°C for the systems 1 and 2 respectively.

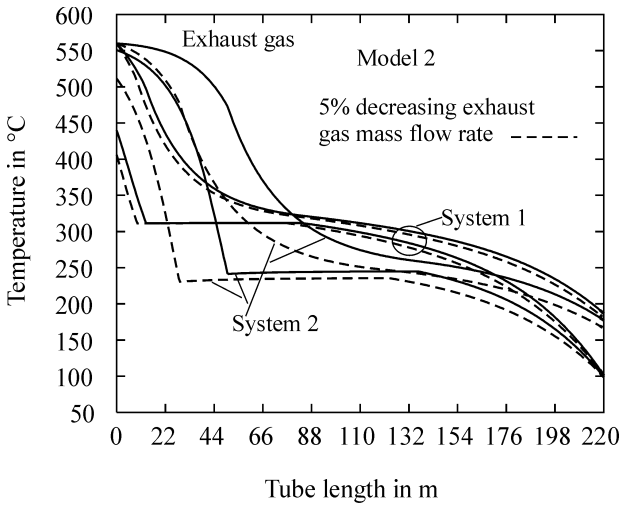


Figure 13: Temperature versus tube length

Concerning the model 3, Fig. 14 shows the reducing of the working fluid temperatures of 2.5% from 530°C for the system 1 and 13% from 300°C for the system 2 at the tube outlets. This is due to a decreasing exhaust gas mass flow rate. The exhaust gas temperatures for the systems 1 and 2 are reduced of 1.7% from 305°C and 2.2% from 217.1°C respectively. Also, for both systems, the outlet exhaust gas temperature shows a decreasing tendency with reducing of the exhaust gas mass flow rate. The corresponding variation of the density on the working fluid side is shown in Fig. 15 for both systems.

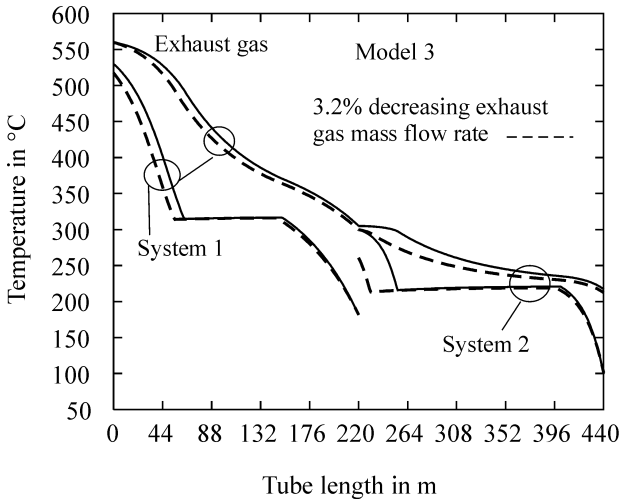


Figure 14: Temperature versus tube length

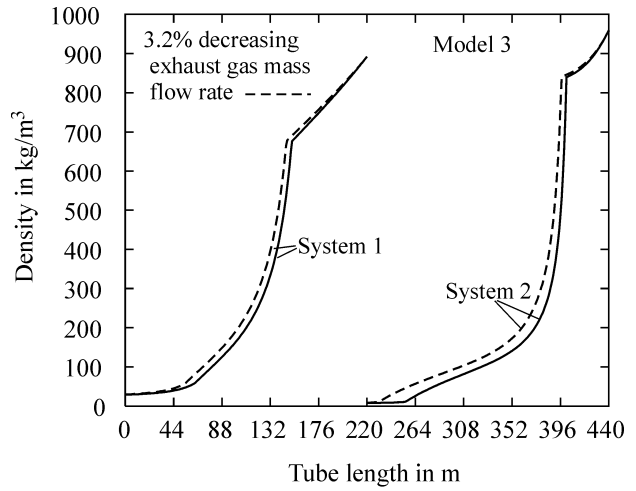


Figure 15: Density versus tube length

4.3 Effect of decreasing exhaust gas temperature

As in the case of decreasing exhaust gas mass flow rate, the reducing of the exhaust gas temperature has an influence on the working fluid parameters for the investigated models. Fig. 16 shows the temperature as function of the tube length for the model 1. There, it is to observe the decreasing working fluid temperatures at the tube outlet of 16.7% from 514°C and 19.7% from 471.8°C for the systems 1 and 2 respectively. The average outlet exhaust gas temperature decreases of 1.1% from 179.7°C. The corresponding curves of the density and steam quality are represented in Figs. 17-18.

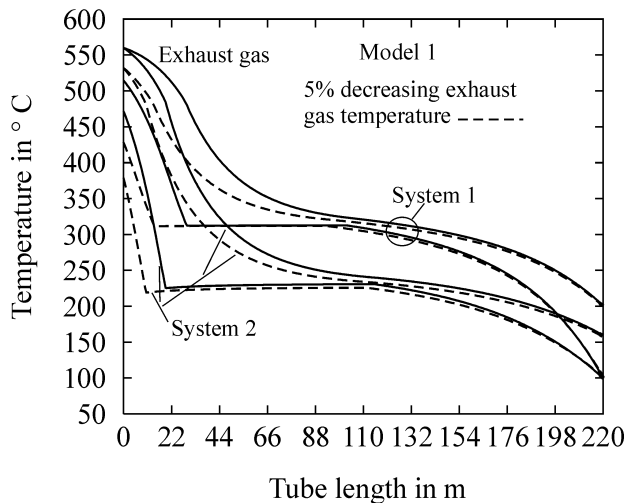


Figure 16: Temperature versus tube length

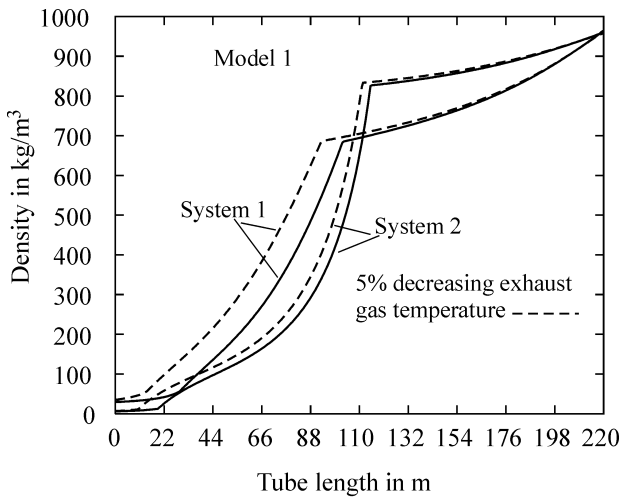


Figure 17: Density versus tube length

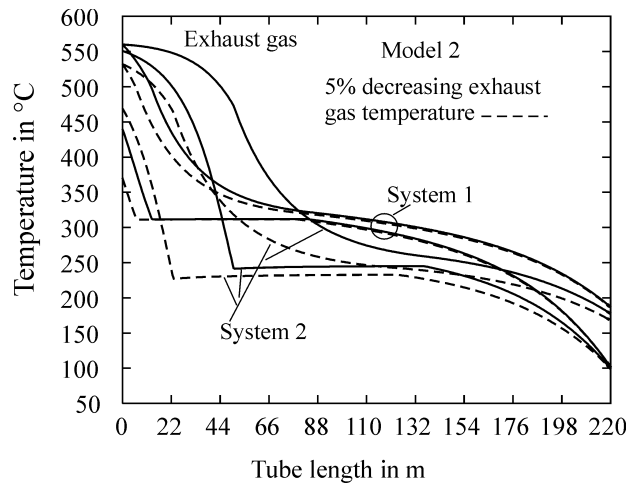


Figure 19: Temperature versus tube length

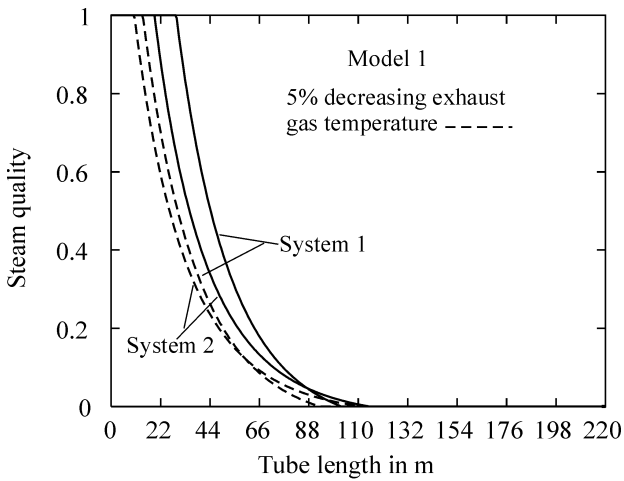


Figure 18: Steam quality versus tube length

Concerning the model 2, Fig. 19 shows the temperature as function of the tube length. From this figure is to see the moving of the boiling zone to the tube outlet with reducing of the exhaust gas temperature. The average outlet exhaust gas temperature decreases of 2.9% from 181.9°C while the working fluid temperatures decrease of 15.8% from 440°C and 14.8% from 550.8°C for the systems 1 and 2 respectively.

In the model 3, the reducing of exhaust gas temperature of 2% leads to a decreasing outlet working fluid temperatures of 4.7% from 530°C for the system 1 and 8.2% from 300°C for the system 2 as represented in Fig 20. The corresponding variation of the steam quality is represented in Fig. 21. Here, it is clearly to observe the displacement of the boiling end point to the tube outlet with the reducing of the exhaust gas temperature.

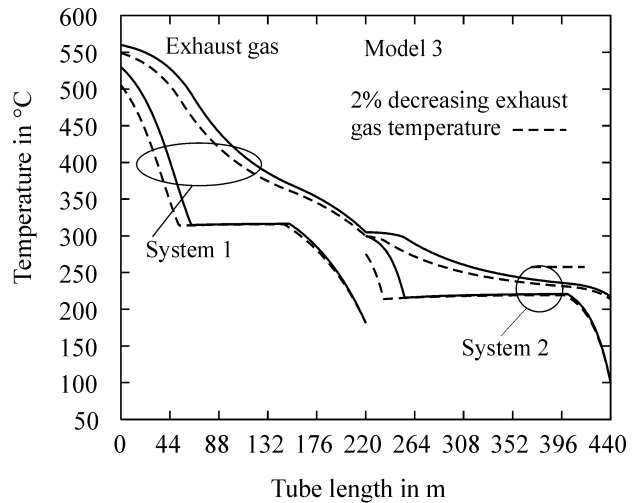


Figure 20: Temperature versus tube length

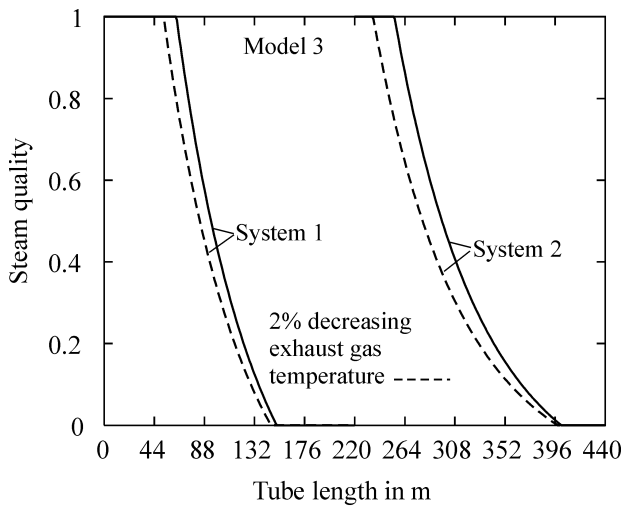


Figure 21: Steam quality versus tube length

4.4 Model comparison

According to the performed investigations, the difference from the three models is clearly observed. The achieved working fluid temperature at the outlet for the system 2 in the model 3 is lower than that for the system 2 in the model 1 and 2 for the same exhaust gas temperature. In spite of the different pressure level of both systems in the models 1 and 2, these models could be suitable used to obtain the almost working fluid temperature at the outlet of both systems. Moreover, in models 1 and 2, a perturbation in working fluid parameters (mass flow rate, pressure, temperature) in a system has no effect on the other system. On the other hand, in the model 3, a reducing or an increase in working fluid parameters in the system 1 strongly affect the system 2, which depends on the heat transfer between the exhaust gas and the system 1.

5. CONCLUSION

In this study three models of a dual-pressure once-through HRSG are developed and examined. They are modeled and simulated considering all relevant physical behaviors in the calculation, i.e. by means of a non-linear mathematical model, a convective heat transfer situation at once-through HRSGs and a slip between water and steam in two-phase flow. This leads to a better understanding of the steady state of heat recovery system with dual-pressure level. The obtained results from the three models clearly show that the variation of the exhaust gas parameters, mainly the temperature and the mass flow rate, strongly affects the operating behavior of the three models. Also, the results reveal the effect of the variation of the tube length on the outlet exhaust gas parameters which present a better tendency with increasing tube length.

ACKNOWLEDGMENTS

The authors are grateful to the Foundation of the University of Quebec in Abitibi-Temiscamingue (FUQAT).

REFERENCES

[1] B. Gericke, Integrated waste heat utilisation in pipeline compressor stations. Part 1: Gas turbines for compressor stations. VGB Power Tech 2/2002, 64-69.

- [2] A. P. Fraas, Heat exchanger design, second edition, John Wiley & Sons, New York, Chichester, Brisbane, Toronto, Singapore, 1989.
- [3] J. S. H. Najjar, Efficient use of energy by utilising gas turbine combined systems, Applied thermal engineering, 21 (2001), 407 – 438.
- [4] R. Kehlhofer, R. Bachmann, H. Nielsen, J. Warner, Combined-cycle gas and steam turbine power plants, Tulsa, Oklahoma / USA, Pennwell publishing company, 1999.
- [5] G. Heyen, B. Kalitventzeff, A comparison of advanced thermal cycles suitable for upgrading existing power plant, applied thermal engineering 19 (1999), 227 – 237.
- [6] A. Franco, A. Russo, Combined cycle plant efficient increase based on the optimization of the heat recovery steam generator operating parameters, International Journal of thermal sciences, 41 (2002), 843 – 859.
- [7] G. D. Ngoma, A. Sadiki, R. Wamkeue, Efficient approach in modelling and simulation of dual pressure once-through heat recovery steam generator, Proceedings of the IASTED Conference, power and energy systems, February 24-26, 2003, Palm Springs, Ca, USA, pp. 218-223.
- [8] Z. Rouhani, Modified correlations for void fraction and two-phase pressure drop. AE-RTV-841, 1969.
- [9] B. Chexall et al., Void Fraction Technology for Design and Analysis, EPRI Electric Power Research Institute, 1997.
- [10] S. Kakaç, A. E. Bergles, F. Mayinger, Heat Exchangers, Thermal-Hydraulic Fundamentals and Design, Advanced Study Institute Book, Berlin Heidelberg, New York, Tokyo, Hemisphere Publishing Corporation, Springer-Verlag, 1980.
- [11] J. P. Holman, Heat transfer, 8th edition, USA: McGraw Hill Companies 1997.
- [12] A. Rolf, Simulation des nichtlinearen, dynamischen Verhaltens von Wärmetauschern sowie ihrer komplexen Schaltungen in Kraftwerksbau mit einem semianalytischen Berechnungsverfahren. Fortschritt-Berichte VDI Reihe 6, VDI-Verlag GmbH, Düsseldorf / Germany, Nr. 141, 1984.
- [13] F. M. White, Fluid Mechanics, fifth edition, McGraw Hill, 2003.
- [14] L. Friedel, Pressure drop during gas/vapour liquid flow in pipes. Int. Chem. Eng. 1980, 20, 352.
- [15] Ingenieure, Verein Deutscher, VDI-Wärmeatlas, Berechnungsblätter für den Wärmeübergang. VDI-Verlag GmbH, Düsseldorf, 8. Auflage, 1997.
- [16] F. Brandt, Wärmeübertragung in Dampferzeugern und Wärmeaustauschern, Band 2, Fachverband Dampfkessel, Behälter und Rohrleitungsbau, 1985.
- [17] E. Schmidt, Properties of Water and Steam in SI-Units, Berlin Heidelberg New York, Springer 1989.